Analysis of the Failure Stress in Pyrotechnically Releasable Mechanical Linking Device

*YeungJo. Lee , DongJin Kim * and .WonGyu. Kang **
*Agency for Defense Development, and Hanwha Corporation **
1 TRC-6-2, ADD, Yusung P.O.B 35-16, Taejeon, Korea
yeungjolee@nate.com

Failure Stress, Ball Type Bolt, Fracture Morphology, FEM Model

Abstract

The present work has been developed the interpretation processor including analysis of the failure stress in pyrotechnically releasable mechanical linking device, which has the release characteristic without fragmentation and pyro-shock, using SoildWorks, COSMOS Works and ANSYS programs. The aim of the invention is to propose a pyrotechnically releasable mechanical linking device for two mechanical elements that does not suffer from such drawbacks. The pyrotechnically releasable mechanical linking device according to the invention is simple, compact and inexpensive in structure. It is simple to implement and permit the use of only a reduced quantity of pyrotechnic composition, such composition possibly being devoid of any primary explosive at all. The present work is only focused on the design of structure and the material characteristics. To analyze the fracture morphology resulted from tensile test in the different ball type bolts, the present work has been performed to estimate the failure stress of material and to make the same result from tensile test. The failure stress of SUS 630 in ductile material is approximately 1050 Mpa. The failure stress of SUS 420 in brittle material is about 1790 Mpa. Among the models used the ductile material, the model 6 is suitable a design of structure compared to that of other models. The use of this interpretation processor developed the present work could be extensively helped to estimate the failure stress of material having a complex geometry such as the ball type bolt

1. Introduction

Explosive bolts are reliable and efficient mechanical fastening devices having the special feature of a built-in release. They are ideally used in space shuttle, missile, aircraft and underwater vehicle systems, for example for launcher operation, stage separation, discharge of external tanks, thrust termination and many other applications [1]. There must be no reconstruct between the separating bodies, no detrimental shock loads induced in the structure, and no excessive or harmful debris.

Numerous different shapes and sizes of explosive bolts have been thus far developed for a great variety of applications. Very careful consideration [2] is required the design factors such as firing characteristics, shape and size, kind of explosive material, quantity of explosive material and environmental conditions under restraint during the time of design of explosive bolt. Two critical design considerations for a release device are the possible shock loading and the damage from debris to adjacent structure. Every effort should be made to select a proven design for a point release device because of the cost and time required to qualify a new design. The recommended type of point-release device is the non-fragmenting assembly, which operates without producing gas and fragments that may damage other parts of the vehicle [3,4].

For maximum reliability, separation mechanisms using mechanical-explosive point-release devices should be designed to contain as few components as possible. All pieces of the separation mechanism should be restrained or captured after separation.

The disadvantage of explosive bolt lies in that it is based on the high explosive effect of a pyrotechnic charge. Indeed, one or several primary explosives are used possibly in association with one or several secondary explosive or energetic but highly confined substances. However, primary explosives are sensitive materials, which are thus difficult or hazardous to implement. So as to ensure the fracture of mechanical support parts the quantities of pyrotechnic charge necessary are also substantial (>100 mg), thereby further increasing the risks and the cost. When the explosive bolt is ignited, there is a risk of fragments of it remaining caught in the different elements thereby perturbing their detachment or separation. The separation effort of the two elements is thus non-reproducible and the device is not reliable enough unless an unacceptably large quantity of explosive is used.

The aim of the present work is to propose a pyrotechnically releasable mechanical linking device for two mechanical elements that does not suffer from such drawbacks. The pyrotechnically releasable mechanical linking device according to the invention is simple, compact and inexpensive in structure. It is simple to implement and permit the use of only a reduced quantity of pyrotechnic composition, such composition possibly being devoid of any primary explosive at all. A standard pyrotechnic initiator can moreover be easily integrated inside the device

according to the present work and this with no modification to its structure. Additionally, the device is reliable and ensures good reproducibility of the separation effects of the mechanical elements.

The present study predicts the failure stress based on fracture morphology of experimental result, performing the interpretation of FEM about six different types of the ball type bolt. The programs used the present work are SoildWorks 2007 and COSMOS Works/ANSYS. It is proved that the interpretation processor approach is an accurate and effective analysis technique for failure model of non explosive actuator. The interpretation processor could be able to make the design of the shape of pyrotechnically releasable mechanical linking device such as the ball type bolt.

2. Design and shape of the ball type bolt

The ball type blot is consisted of initiator, housing, body, pin and balls as shown in Fig. 1. It shows three-dimension model of ball type bolt as shown in Fig. 2.

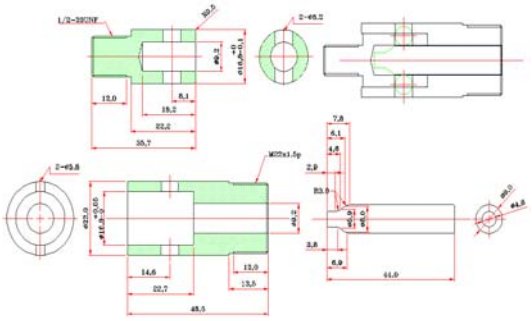

Fig.1. Two dimension drawing of ball type bolt

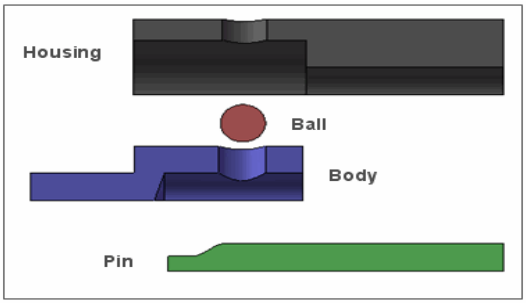

Fig.2. Three dimension shape of ball type bolt

3. Tensile test of the ball type bolt

The tensile test was carried out four different types of the ball type bolt according to KS B 0800 2003. Table 1 represents the tensile load of four different models when the ball type bolt is fractured. Materials used the present work were applied STS 630(ductile) and STS 420(brittle) for housing, body and pin. The ball material was used the super-alloy which has a higher than the ultimate tensile stress of STS 630. Table 2 shows materials used the present work

Table 1 Tensile property of four different models.

	Tensile Load [kgf]			Test Method
	Test 1	Test 2	Avg.	
Model 1	8,411	8,604	8,507	KS B
Model 2	6,698	6,428	6,563	KS B
Model 3	7,475	7,328	7,401	KS B
Model 4	9,908	10,651	10,279	KS B

Table 2 Materials used the present study

	Model1	Model2	Model3	Model4
Housing	SUS630	SUS420	SUS420	SUS 630
Body	630	420	630	630
Pin	630	420	630	420
Ball	Rigid	Rigid	Rigid	Rigid

When the ball type bolt was tested the tensile load, the fracture was initiated at the housing part and fracture mode was appeared differently according to material used. Figure 3 shows the fracture morphology of four different samples resulted in tensile tests.

(a) Model 1

(b) Model 2

(c) Model 3

(d) Model 4

Fig. 3 Fracture morphology of four different models

4. Model of failure analysis

Applying tensile test, the failure was occurred at contact plane between the housing section and the ball. The estimation of failure through the interpretation of FEM was carried out only the housing part in the ball type bolt, and the theory of failure estimation was applied differently according to materials. In the SUS 630 case (ductile), Maximum von-mises stress is used to failure stress which has been based on the theory of failure estimation for ductile material. The equation is as follows;

$$\frac{\sigma_{von-mises}}{\sigma_{yield}} < 1 \qquad (1)$$

To predict the failure stress of the SUS 630 material, the level of applied stress in the fracture plane as shown in Fig. 4 exceeds. Assuming this material is fractured, the level of applied stress selected the yield stress of the SUS 630 material.

Fig. 4 Standard of failure estimation in ductile material

In the SUS 420 material (brittle), the maximum normal stress was used to as the failure stress, which has been based on the theory of failure estimation for brittle material. The fracture is caused when reached the ultimate tensile stress of each component material.

$$\frac{\sigma_1}{\sigma_{UTS}} < 1 \qquad (2)$$

If the level of applying stress in the whole of fracture plane as shown in Fig. 5 exceeds completely, the material could be fractured. To predict the failure stress of the SUS 420 material, the level of applying stress selected the ultimate tensile stress of the SUS420 material.

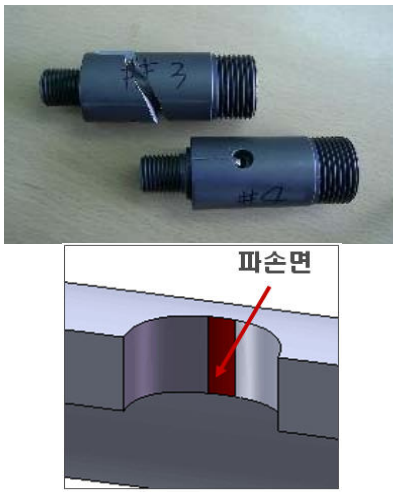

Fig. 5 Standard of failure estimation in brittle material

5. Interpretation of finite element method

5. 1 Material condition

The interpretation was carried out the stress analysis of the ball type bolt to consider the linear static with contact between the part and the part. The mechanical properties [5] used in the present work arrange in tables 3 and 4. The interpretation was used the elastic modulus and ν of each material, the value of the ultimate tensile stress and the yield stress applied to estimate the failure stress. The elastic modulus of ball material is considered to be more than decuple those of the housing and the pin material.

Table 3 Mechanical properties of SUS 420 material

SUS 420	E[Gpa]	v
AISI T 420 SS	200	0.24
AISI T 420 SS (Tempered)	200	0.24

SUS 420	UTS [Mpa]	Yield [Mpa]	El (%)
AISI T 420S SS	2,025	1,360	2.5%
AISI T 420 SS (Tempered)	1,702	1,380	7%

Table 4 Mechanical properties of SUS 630 material

SUS 630	E [Gpa]	v
SUS 630, SS 900	197	0.272
SUS 630, SS1100	197	0.272

SUS 630	UTS [Mpa]	Yield [Mpa]	Elongation (%)
SUS630, SS900	1,365	1,262	15%
SUS630, SS1100	1,034	931	17%

5. 2 Model of finite element method

Creating a model of shape is used SolidWorks and whole assembly is made from a model of ball type bolt consists of individual item. Fig. 6 appears the assembly cutting one quarter to rotation direction, in model 1, and they are also represented with the finite element method. Table 5 represents the total of element and point used the six different models.

Table 5 Element and point used the present models

	Model 1	Model 2	Model 3
element	106,930	44,426	63164
point	567,322	222,075	327,630

	Model 4	Model 5	Model 6
element	73,060	120,409	43,436
point	381,913	646,299	219,471

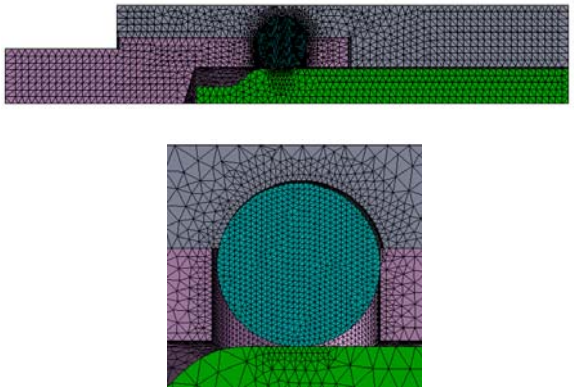

Fig. 6 FEM modeling of model 1

5. 3 Condition of load/restriction

The condition of restriction used the present work applied the symmetrical condition to one quarter to rotation plane as shown in Fig. 7, the right side of the housing and pin was restricted completely. The condition of contact between the each parts was used basically point-point contact, but some model was applied the condition of plane–plane contact. The condition of load was used the quarter value of mean tensile stress. In the SUS 630 material, as the fracture was initiated at the 80% value of tensile load, the models 1, 4, 5 and 6 used the SUS 630 material were applied the 80% value of tensile load. Table 6 shows the applying load of each model.

5. 4 Result

The present interpretation is applied a linear model and failure model applied differently to the characteristic of material. The distribution of stress in each model is used to confirm the location originated the maximum stress.

Table 6 Appling load of each model

	Model 1	Model 2	Model 3
Load [kgf]	2,126 *80% **=1,700**	**1640.75**	**1850.375**
	Model 4	Model 5	Model 6
Load [kgf]	2569.88 *80% **=2,055**	2569.88 *80% **=2,055**	2569.88 *80% **=2,055**

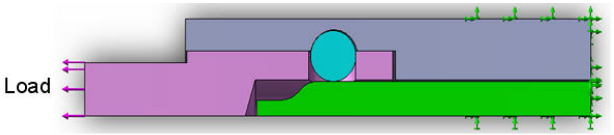

Fig. 7 Condition of load and restriction

5. 4. 1. Model 1

The distribution of equivalent stress shows the whole distribution of stress as shown in Figs 8 and 9. The Maximum von-mises stress is applied to the housing.

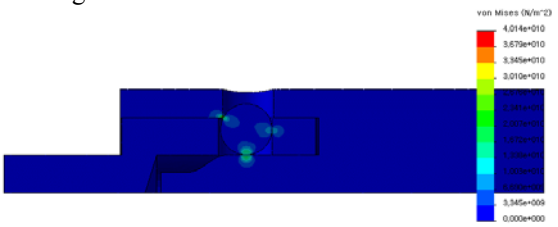

Fig. 8 The whole distribution of equivalent stress in model 1

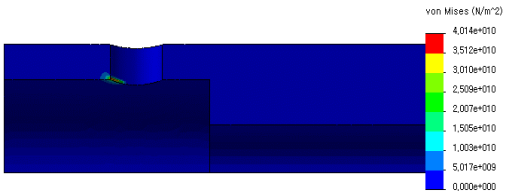

(a) Housing

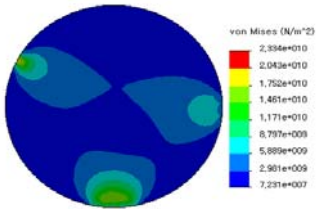

(b) Ball

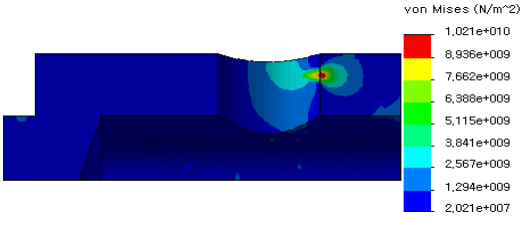

(c) Body

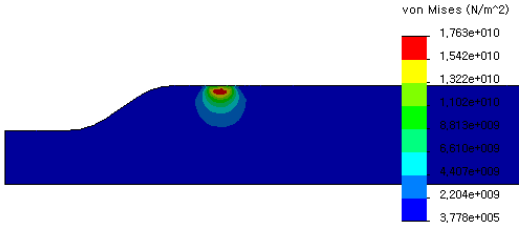

(d) Pin

Fig. 9 The distribution of equivalent stress in each part

The housing in model 1 which has the ductile material (SUS630) is estimated to base on the Maximum von-Mises stress. The size of ball is 6 mm and the location of ball is opened fully as shown in Fig. 8. Fig. 10 shows the fracture morphology in model 1. Figure 11 represents the distribution of calculated stress. The failure stress predicts to control the range of stress to have the range of stress similar to the fracture morphology. Figure 12 shows only the section of the two colors based on the predicting failure stress to understand the failure stress. As shown in Fig. 12, the failure stress of housing in model 1is predicted to be a 1050 Mpa.

Fig. 10 Fracture morphology of model 1

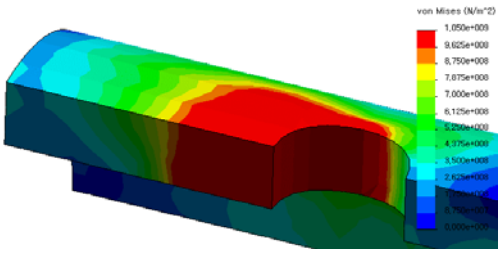

Fig. 11 The distribution of equivalent stress in housing

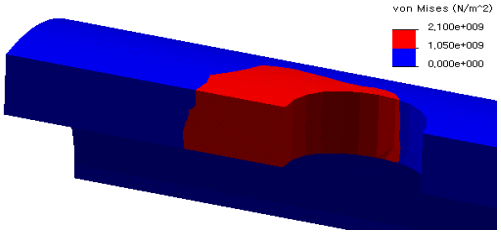

Fig. 12 Failure estimation of housing (model 1)

5. 4. 2 Model 2

The whole components were used the SUS420 material. The size of ball is 6 mm and the location of ball is opened fully as shown in Fig. 13. The distribution of stress shows the distribution of principle stress shown in Figs. 13 and 14. The principal stress is applied the housing.

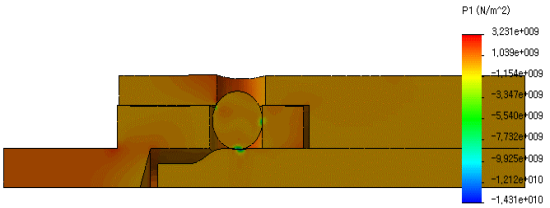

Fig. 13 The distribution of principal stress in model 2

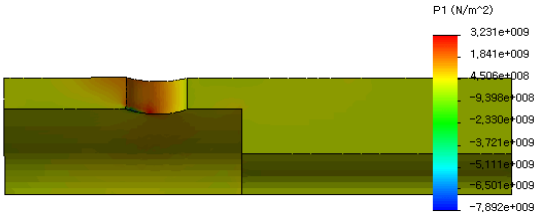

(a) Housing

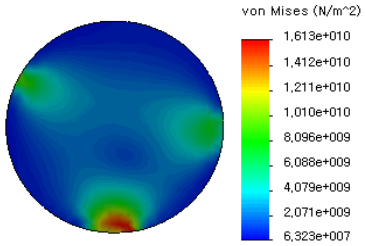

(b) Ball

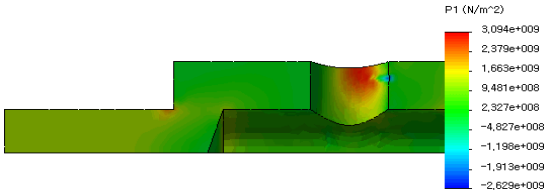

(c) Body

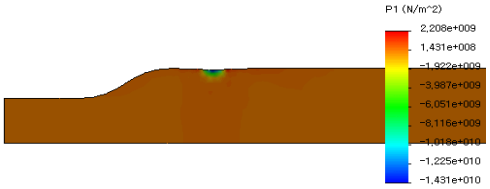

(d) Pin

Fig.14 The distribution of principal stress in each part

Figure 15 shows the fracture morphology of model 2 and Fig. 16 appears the distribution of calculated principal stress. The failure stress predicts to control the range of stress to have the tress range similar to stress occurred the fracture morphology. Fig. 17 shows the section of two colors based on the predicting failure stress to represent failure stress. The failure stress of housing in model 2 is predicted to be a 1730 Mpa.

Fig.15 Fracture morphology of model 2

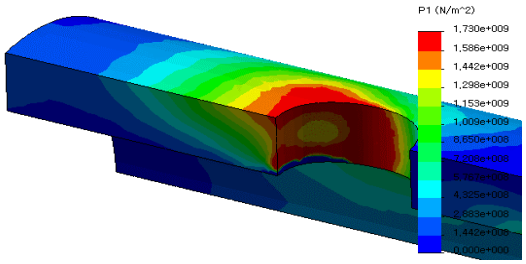

Fig. 16 The distribution of principal stress in housing (model 2)

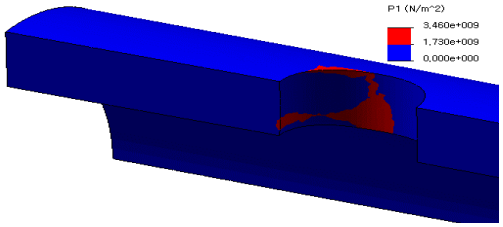

Fig. 17 The estimation of failure in housing (model 2)

5. 4. 3 Model 3

In the model 3, housing and other parts are consisted of SUS 420material (brittle) and SUS 630 material (ductile) respectively. The size of ball is 6 mm and the location of ball is opened fully as shown in Fig. 18. The failure estimation is used the distribution of principal stress in model as shown in Figs 18 and 19, as housing is made of the SUS 420 material. The principle stress was occurred at housing (contact plane between housing and ball)

Fig. 18 The distribution of principal stress in model 3

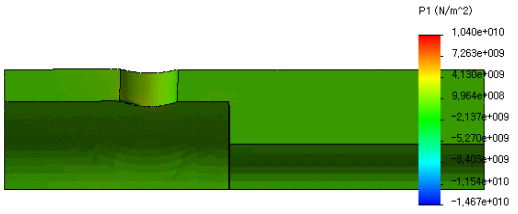

(a) Housing

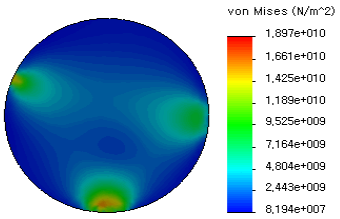

(b) Ball

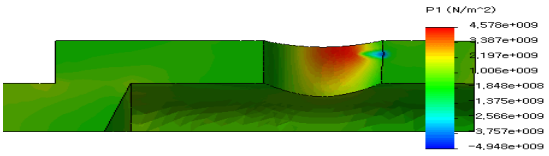

(c) Body

(d) Pin

Fig.19 The distribution of principal stress in each part

Figure 20 shows the fracture morphology of model 3. Fig. 21 appears the distribution of calculated principle stress. The failure stress predicts to control the range of stress to have the tress range similar to stress occurred the fracture morphology. Fig. 22 shows the section of two colors based on the predicting failure stress to represent failure stress. The failure stress of housing in model 3 is predicted to be a 1850 Mpa.

Fig. 20 Fracture morphology of model 3

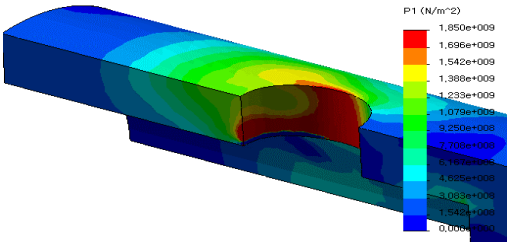

Fig. 21 The distribution of principal stress in housing (model 3)

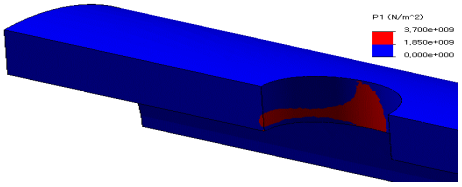

Fig. 22 Failure estimation of housing (model 3)

5. 4. 4 Model 4

In the model 4, housing including body and pin consist of SUS 630 (ductile) material and SUS 420 (brittle) material respectively. The size of ball is 6 mm and the location of ball is not opened fully as shown in Fig. 23. The failure estimation is used the distribution of the Maximum von-Mises stress in model as shown in Figs. 23 and 24 , as housing is made of the SUS 420 material. The Maximum von-Mises stress was occurred at housing (contact plane between housing and ball).

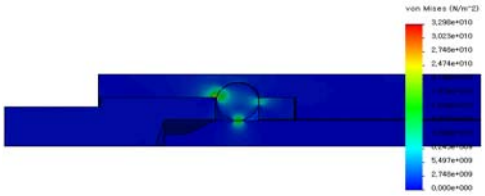

Fig. 23 The whole distribution of equivalent stress in model 4

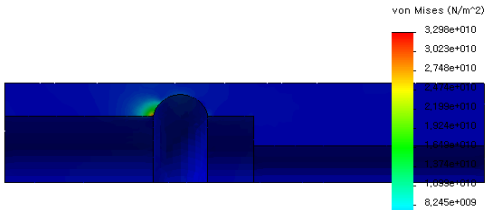

(a) Housing

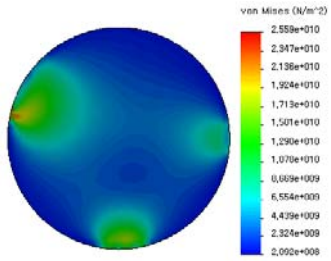

(b) Ball

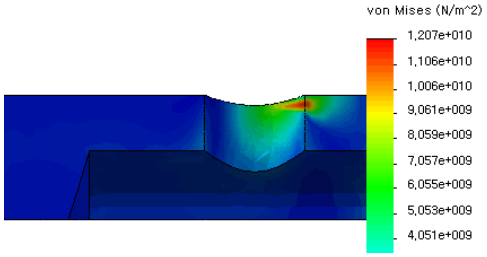

(c) Body

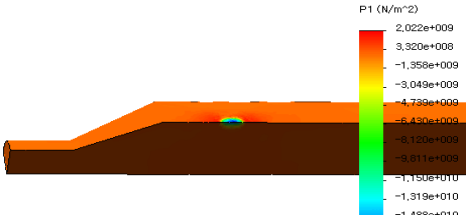

(d) Pin

Fig. 24 The distribution of equivalent stress in each part

Figure 25 shows the fracture morphology of model 4. Figure 26 appears the distribution of calculated Maximum von-Mises stress. The failure stress predicts to control the range of stress to have the tress range similar to stress occurred the fracture morphology. Figure 27 shows the section of two colors based on the predicting failure stress to represent failure stress. The failure stress of housing in model 3 is predicted to be a 2250 Mpa

Fig. 25 Fracture morphology of model 4

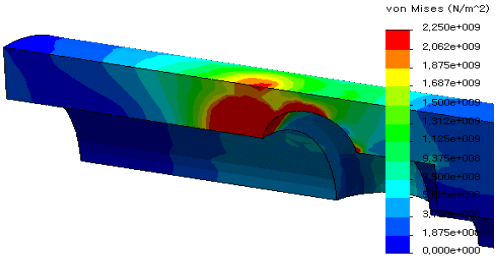

Fig. 26 The distribution of Maximum von-Mises stress in housing (model 4)

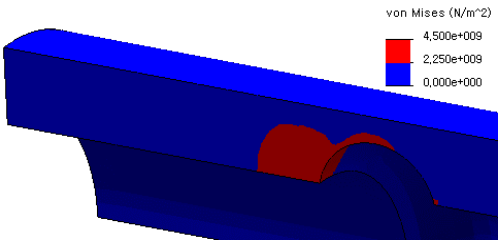

Fig. 27 Failure estimation of housing (model 4)

5. 4. 5 Model 5

In the model 5, housing and body are used SUS 630 (ductile) material and pin is used SUS 420 (brittle) material. The size of ball is 8 mm and the location of ball is not opened fully as shown in Fig. 28. The failure estimation is appeared the distribution of the Maximum von-Mises stress in model 5 as shown in Figs. 28 and 29, as housing is made of the SUS 420 material. The Maximum von-Mises stress was occurred at housing (contact plane between housing and ball).

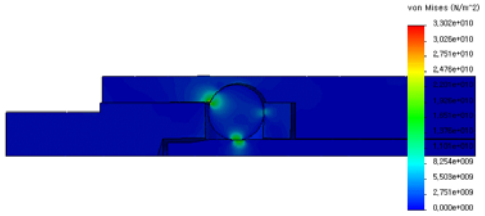

Fig. 28 The whole distribution of equivalent stress in model 5

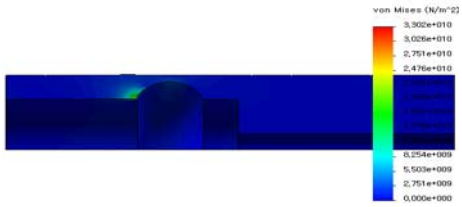

(a) Housing

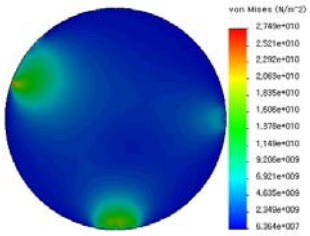

(b) Ball

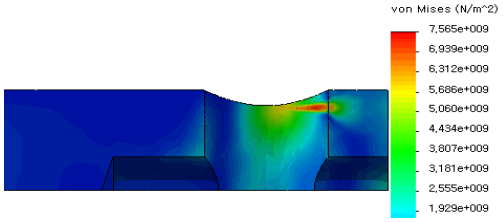

(c) Body

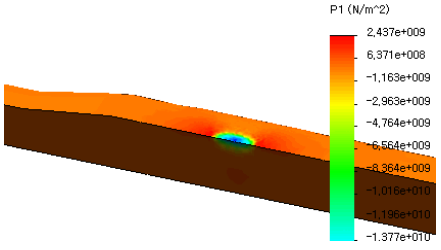

(d) Pin

Fig. 29 The distribution of equivalent stress in each part

In the model 5, the failure stress is not possible to predict based on fracture morphology because tensile test was not carried out. Thus the fracture morphology is predicted to use the calculated failure stress from model 1 and model 4 used SUS 630 as housing material. Figures 30 and 31 show the fracture morphology based on model 1 (failure stress 1050 Mpa) and model 4(failure stress 2250 Mpa) respectively.

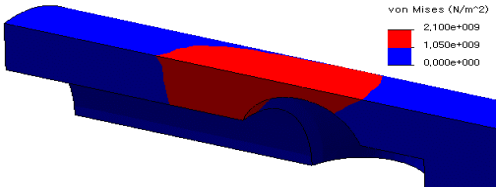

Fig. 30 Fracture model in model 5 based on model 1

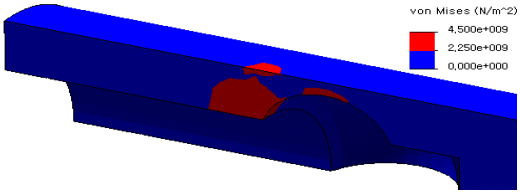

Fig. 31 Fracture model in model 5 based on model 4

5. 4. 6 Model 6

In the model 6, housing and body are used SUS 630 (ductile) material and pin is used SUS 420 (brittle) material. The size of ball is 4 mm and the location of ball is not opened fully as shown in Fig. 32. The failure estimation is appeared the distribution of the Maximum von-Mises stress in model as shown in Figs 32 and 33, as housing is made of the SUS 420 material. The Maximum von-Mises stress was occurred at housing (contact plane between housing and ball)

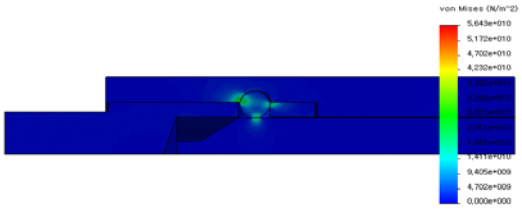

Fig. 32 The distribution of equivalent stress in model 6

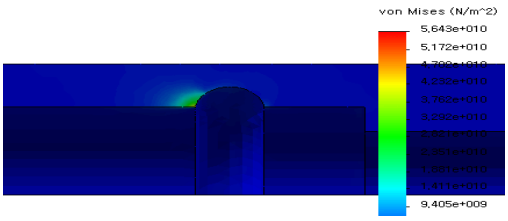

(a) Housing

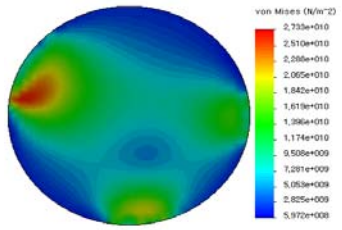

(b) Ball

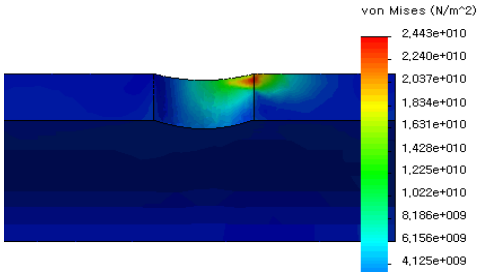

(c) Body

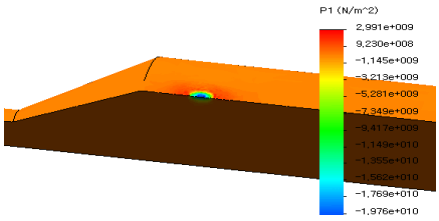

(d) Pin

Fig. 33 The distribution of equivalent stress in each part

In the model 6, the failure stress is not possible to predict based on fracture morphology because tensile test was not carried out. Thus the fracture morphology is predicted to use the calculated failure stress from model 1 and model 4 used SUS 630 as housing material. Figures 34 and 35 show the fracture morphology based on model 1 (failure stress 1050 Mpa) and model 4 (failure stress 2250 Mpa) respectively.

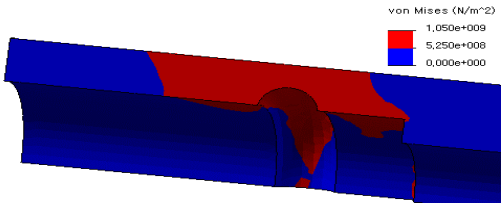

Fig. 34 Fracture model in model 6 based on model 1

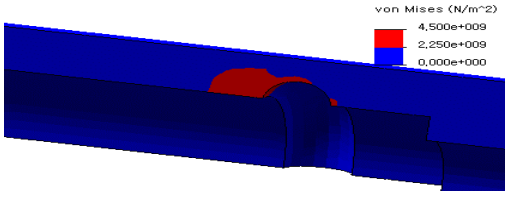

Fig. 35 Fracture model in model 6 based on model 4

5. 4 Discussion

The failure stress of model 2 and model 3 in brittle material is 1730 Mpa and 1850 Mpa respectively. The failure stress of model 1 and model 4 in ductile material is 1050 Mpa and 2250 Mpa respectively. In the case of ductile material, the predicting failure stress of model 1 and model 4 is seen to be over the 100% of error. It is caused from the characteristic of ductile material. The present interpretation was not considered a nonlinear feature of mechanical property but a linear feature. Even the failure stress is over the yield stress, the failure stress will be calculated from the elastic modulus of this material. The elastic modulus within the region of plastic deformation in ductile material has the value between 1/500 and 1/1000. Thus the yield stress of SUS 630 material may be a 1052 Mpa as shown in Fig. 36, it is very similar to that of model 1.

In the present work, it can be predicted that the ultimate tensile stress of SUS 420 material is about a 1790 Mpa and the yield stress of SUS 630 material is about a 1050 Mpa.

Comparing the model 2 and model 3 in the brittle material, the interpretation of FEM is quietly similar to those of the failure stress and the distribution of principal stress. Comparison of model 4, model 5 and model 6 used the ductile material has been shown some different result that the distribution of Maximum von-Mises stress in model 6 is best than that of model 4 and model 5 as shown in Figs. 27, 31 and 35. So if it is used to the ductile material as the housing part, model 6 could be a suitable one. The 4 mm of ball is best compared to the 6mm and 8 mm of ball.

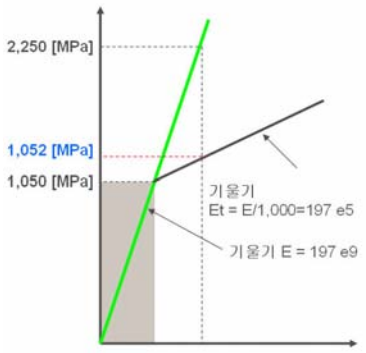

Fig. 36 The supplementary correction of yield stress in ductile material

6. Conclusions

To analyze the fracture morphology resulted from tensile test in the different ball types bolt, the present work has been performed to estimate the failure stress of material to make the same result from tensile test.

The predicting failure stress may be confirmed within the range of the ultimate tensile stress and the yield stress in tables 3 and 4. In result of interpretation,

the failure stress of the housing may be predicted as follows;

1) The failure stress of SUS 630 in ductile material is approximately 1050 Mpa
2) The failure stress of SUS 420 in brittle material is about 1790 Mpa
3) Among the models used the ductile material, the model 6 is very good concerning the distribution of Maximum von-Mises stress, So the failure stress in model 6 is larger than that of model 4 and model 5.
4) The failure stress calculated from the present work can be applied to the material model of the ball type bolt, in pyrotechnically releasable mechanical linking device.

7. References

1) Brauer, K. O.: *Handbook of Pyrotechnics*, Chemical Publishing Co. Inc., NY, 1974, pp 119-128.
2) Cole, J. K. and Wolfe, W. P.: ASP Base Plate Design and Explosive Bolt Test, Sandia Report, SAND 88-2543, 1988.
3) Lee, Y. J.: The Study of Development of Ridge-Cut Explosive Bolt (I), ADD Report, TEDC-421-000939, 2000, pp. 1-63.
4) Meyer, M. A. and Murr, L. E.: *Shock Wave and High-Strain-Rate Phenomena in Metals*, Plenum Press, NY, 1981, pp. 51-63.
5) Metal Handbook Twenty Edition, Volume 1, “Properties and Selection: Irons and Steels”, 1998.